

## Equilibrium Considerations in the Methane Synthesis System

Gerald Gruber

FMC Corporation, Princeton, N. J.

### Summary

An investigation was made into the equilibria of the methanation reaction, coupled with the shift reaction and the carbon deposition reaction. Of particular interest is the exploration of regions where carbon deposition is possible according to thermodynamic criterion, assuming that carbon is deposited as graphite or "Dent" carbon.

The carbon laydown curves are plotted on a unique coordinate system which corresponds to starting composition variables that are commonly used. The effects of pressure, temperature and starting composition on carbon laydown are investigated over a wide range of practical interest, and beyond. All possible starting compositions are considered over a temperature range of 600°K (625°F) to 2000°K (3140°F) and a pressure range of 30 atm (426 psig) to 300 atm (4395 psig). In addition, the effects of pressure, temperature and starting composition on equilibrium composition and product gas heating value are examined. The figures presented provide a useful tool for the rapid scanning of the effect of possible starting gas composition, pressure and temperature on product gas quality and useful operating regions. The utility of the graphs are not limited to a single stage reaction, but can be used for multiple stage reactors with arbitrary amounts of diluents ( $H_2O$ ,  $CO_2$ ,  $CH_4$ ) and recycle gas, which may change from stage to stage. Additionally, the pressure and temperature of each stage may be considered independently.

## Equilibrium Considerations in the Methane Synthesis System

Gerald Gruber

FMC Corp., Princeton, N. J.

Introduction

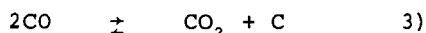
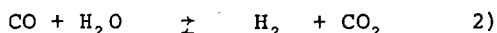
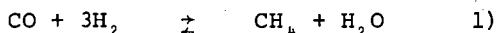
Considering the synthesis of methane from carbon monoxide and hydrogen, it is desired to operate a reactor, or reactors, in such a way as to avoid the deposition of carbon on catalyst surfaces and to produce a high quality product gas. Since gas compositions entering the reactor may vary considerably because of the use of diluents and recycle gas in a technical operation, it is desirable to estimate the effects of initial gas composition on the subsequent operation. Pressure and temperature are additional parameters.

It is a simple enough matter to calculate the equilibrium composition for any given starting composition, pressure and temperature. It is no more difficult to do it for a range of starting compositions, pressures and temperatures, except that it takes longer. Since the calculations are done on a computer, many parameters can be closely examined. However, faced with the great mass of calculated results, it is important to have them presented in a concise, informative manner.

By using a particular type of triangular diagram, it is possible to represent all possible starting compositions of CO, CO<sub>2</sub>, H<sub>2</sub>, H<sub>2</sub>O and CH<sub>4</sub> on a single coordinate system which is easy to use.

Chemistry

Consider the following reactions which are sufficient to describe the system:



In addition, it will be convenient to make reference to another reaction:



which is not independent of reactions 1-3.

Reactions 1 and 3 are highly exothermic and therefore have equilibrium constants that decrease rapidly with temperature. Reaction 2 is moderately exothermic, and consequently its equilibrium constant shows a moderate decrease with temperature. Reaction 4 is moderately endothermic and its equilibrium constant increases with increasing temperature.

The relationship between temperature and equilibrium constant for these four reactions is indicated in Figure I, where carbon is assumed to be graphite. Thermodynamic data were taken from JANEF (1) and Rossini (2).

If we allow for the fact that carbon may be deposited in a form other than graphite, the equilibrium constants of reactions 3 and 4 must reflect the different state. This behavior has in fact been observed by Dent (3).

Dent and his coworkers found that the observed equilibrium constant for reaction 3 was less than the theoretical equilibrium constant for deposition of graphite based on measurements made between 600°K and 1200°K. The departure was greatest at 600°K, and the observed and theoretical equilibrium constants approached each other as the temperature increased, becoming equal at about 1100°K to 1200°K. The difference in free energy between graphite and the actual form of carbon deposited was also determined by decomposing pure  $\text{CH}_4$  and by depositing carbon from a  $\text{CO}$  and  $\text{H}_2$  mixture. These results confirmed the measurements made by decomposing pure  $\text{CO}$ . These experiments were performed over a nickel catalyst and it is speculated that the anomalous free energy of the deposited carbon may be due to the fact that it forms a carbide or a solid solution.

Whatever the exact form of the carbon deposition is, it must be recognized and taken into account in future calculations. The deposited material is called "Dent" carbon, and equilibrium constants based on its free energy are also indicated in Figure I. The fact that carbon deposits as "Dent" carbon has been qualitatively confirmed by Pursley (4).

Other recent equilibrium calculations (5, 6, 7) found in the literature assume carbon deposition to be in the form of graphite. In this paper, calculations are based on both cases, graphite and "Dent" carbon.

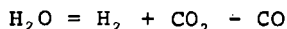
#### Calculation of Carbon Deposition

If we consider the system consisting of the six species,  $\text{CO}$ ,  $\text{H}_2$ ,  $\text{H}_2\text{O}$ ,  $\text{CO}_2$ ,  $\text{CH}_4$ , and  $\text{C}$ , together with the three independent reactions 1 through 3, the system can be uniquely defined by specifying three species. As a matter of convenience, we

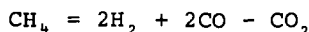
select the three species to be  $H_2$ ,  $CO$ , and  $CO_2$ , and furthermore, by normalizing the composition such that the number of moles of the species sums to unity we only have to specify two species explicitly, which are chosen to be  $H_2$  and  $CO$ . Then, the composition of  $CO_2$  is implied. In order to calculate carbon deposition, for any given starting temperature the procedure is to solve equations 1 and 2 for the equilibrium composition, ignoring carbon deposition. After the equilibrium composition is obtained, a check is made to see if the ratio  $(CO)^2/CO_2$  according to equation 3 would lead to carbon deposition. If no carbon deposition is indicated, then the entire calculation is repeated using equations 1 to 3 if it is desired to calculate the amount of carbon deposited. By using the above procedure, a line is defined which defines the coordinate region into two areas; one where graphite may deposit, and one where graphite may not deposit - based on equilibrium calculations. A sample of this type of graph is shown in Figure II.

#### Coordinate Systems

Before we discuss the curves in Figure II, a short discussion of the coordinate system will be presented. As indicated above, any possible composition of  $CO$ ,  $CO_2$ ,  $H_2$ ,  $H_2O$ , and  $CH_4$  (solid carbon also) may be depicted on the coordinate system shown if the independent species are selected to be  $H_2$ ,  $CO$  and  $CO_2$ . Further, the sum of the species is set to unity and only  $H_2$  (Y coordinate) and  $CO$  (X coordinate) are explicitly plotted. Pure  $H_2$  is indicated as the point (0, 1.0) and pure  $CO$  is indicated at the point (1.0, 0). Similarly, pure  $CO_2$  is at the point (0, 0), and compositions corresponding to pure  $H_2O$  (-1, 1) and pure  $CH_4$  (2/3, 2/3) are also indicated. Water, for example, in terms of the independent species is expressed as



as the point on the graph corresponds to  $X = 1$  and  $Y = 1$ . Similarly,  $CH_4$  may be expressed as



The total number of moles is 3 so that upon normalizing  $Y = 2/3$  and  $X = 2/3$ . In general, for a mixture of arbitrary composition, the coordinates are given by

$$Y = \frac{H_2O + H_2 + 2CH_4}{H_2O + H_2 + CO_2 + CO + 3CH_4} \quad 5)$$

$$X = \frac{CO - H_2O + 2CH_4}{H_2O + H_2 + CO_2 + CO + 3CH_4} \quad 6)$$

Furthermore, compositions may be found graphically by a lever rule. All mixtures of pure  $\text{CO}_2$  and pure  $\text{H}_2$  fall along the Y axis, the distance from pure  $\text{CO}_2$  being inversely proportional to the amount of pure  $\text{CO}_2$  in the mixture. Similar rules hold for any pair of pure components or, in fact, for any pair of mixtures, with the exception of methane, or mixtures containing methane. Since one mole of methane is equivalent to 3 moles of independent species, methane concentrations must be weighed by a factor of three.

Generally speaking, the area of physical reality corresponds to the region bounded by the straight lines connecting the pure components on Figure II. The region formed to the right of  $\text{CH}_4 - \text{CO}$  line and below the extension of the  $\text{H}_2\text{O} - \text{CH}_4$  line corresponds to mixtures of  $\text{CH}_4$ ,  $\text{CO}$  and solid C, and, although physically realizable, is not considered here.

The two curves shown in Figure II divide the graph into graphite forming and non-graphite forming regions. These curves are for 30 atm pressure and for  $650^\circ\text{K}$  and  $750^\circ\text{K}$ , conditions which are typical of many proposed methanation processes (4, 8, 9, 10). The region below and to the right of the curve is where graphite might be deposited.

Consider the point A on Figure II corresponding to a stoichiometric mixture of  $\text{H}_2$  and  $\text{CO}$ . If pure  $\text{CO}_2$  is added to the mixture, the point C may be reached by moving along the line connecting the point and pure  $\text{CO}_2$ . Similarly, if pure  $\text{H}_2\text{O}$  is added, the composition moves along the line connecting point C and pure  $\text{H}_2\text{O}$  until the point D is reached. Point B can be reached by adding  $\text{H}_2$  and removing  $\text{H}_2\text{O}$ , which point incidently corresponds to a stoichiometric mixture of  $\text{H}_2$  and  $\text{CO}_2$ , or it may be viewed as a stoichiometric mixture of  $\text{H}_2$  and  $\text{CO}$  with an excess of water.

Suppose a starting mixture corresponding to point A, is allowed to react according to equation 1 to produce some  $\text{CH}_4$  and  $\text{H}_2\text{O}$ . The composition of this new mixture is still represented by point A. If water is now removed from the mixture, the composition moves along the line connecting point A and pure  $\text{H}_2\text{O}$  to a point E. The extension of this line intersects the point for pure  $\text{CH}_4$ . If the mixture, whose composition is represented by E, is allowed to react further, and if the water produced is subsequently removed, the point representing the composition will move along the line A - E getting closer to pure  $\text{CH}_4$ .

One objective is to approach pure methane without causing the deposition of carbon or graphite, and these curves provide a rapid picture of how this may be done by operating at different starting compositions and temperatures, even with multiple stages.

Let us now focus attention on the curves in Figure II. Either one will serve as a basis for a qualitative discussion. Consider first mixtures of pure CO and  $\text{CO}_2$ , all points of which lie on the X axis. The equilibrium in this system is fully described by equation 3. As the temperature increases, the equilibrium constant decreases, and CO becomes stable. At the temperature considered here, the mixture will deposit graphite until almost pure  $\text{CO}_2$  is reached. Thus the graphite deposition curve will intersect the X axis at a point which is very close to  $X = 0$  (at  $750^\circ\text{K}$  it is approximately  $X = .01$ ). Pure  $\text{CO}_2$  is stable with respect to carbon deposition, as is pure  $\text{H}_2$ , but there is a large composition range where mixtures of  $\text{H}_2$  and  $\text{CO}_2$  will deposit graphite. Thus the carbon deposition curve intersects the Y axis at two points, as indicated on Figure II. In the region of pure  $\text{CH}_4$ , the equilibrium is governed by equation 4. For this reaction, the equilibrium constant increases with temperature so that at high enough temperatures there will be appreciable dissociation  $\text{CH}_4$  to  $\text{H}_2$  and graphite. In the temperature range considered here, the thermodynamic equilibrium indicates only a very small amount of dissociation so the intersection of the graphite deposition curve and the  $\text{H}_2 - \text{CH}_4$  line occurs at almost pure  $\text{CH}_4$ . As the temperature increases, the point of intersection will move towards pure  $\text{H}_2$  on the  $\text{H}_2 - \text{CH}_4$  line.

So far, we have discussed graphite deposition only in terms of the two reactions 3 and 4. As the temperature increases, graphite deposition by reaction 4 is favored, and is retarded by reaction 3. The net result is that the graphite deposition curves for two temperatures will intersect at some point. This will become clearer when we consider curves at different temperatures than indicated here.

### Carbon and Graphite Deposition

#### A. Pressure

In Figure II, curves for two temperatures have been presented that indicate the areas of graphite deposition. Before we consider the effects of higher temperatures, the effect of pressure will be examined.

Figure III shows the graphite deposition curves for 3 pressures at  $700^\circ\text{K}$ . This graph uses the same coordinate system, but is plotted on a larger scale. Again we start by considering the effects of pressure on the two, 2-component systems represented by reaction 3 in one case, and by reaction 4 in the other case.

An increase in pressure favors the reverse of reaction 4 which has the effect of decreasing the graphite formation area in the vicinity of pure methane. Thus the intersection of the graphite deposition curve and the pure  $H_2 - CH_4$  line moves toward pure  $CH_4$ . In considering reaction 3, an increase in pressure enhances the deposition of graphite and the intersection of the graphite deposition curve and the X axis will move closer to pure  $CO_2$ . This behavior again leads to an intersection of the graphite deposition curve for two different pressures. For the temperature indicated ( $700^\circ K$ ), the effect of pressure on the location of the graphite deposition curve is not large, although the effect is more pronounced at higher temperatures.

#### B. Temperature

Attention will now be focused on the effect of temperature on the graphite deposition curve, considering a larger temperature range and the deposition of "Dent" carbon.

Figure IV shows the graphite deposition curves for the temperature range of  $650^\circ K$  to  $2000^\circ K$ . The upper temperature is far above the maximum capability of catalysts which are being proposed to carry out the methanation reaction on a large scale (6); however, it is interesting to carry out the calculations to these high temperatures, assuming that no other reactions will take place.

The behavior previously discussed is now more evident. Along the X axis, as the temperature increases, the intersection of the graphite deposition curve moves towards pure  $CO$ , while along the  $H_2 - CH_4$  line the intersection moves towards pure  $H_2$ . Thus, the odd result appears that as the temperature increases, graphite deposition is less likely for starting mixtures which are near stoichiometric, but it is more difficult to produce pure methane by removing water and reacting the mixture further. Due to equilibrium considerations, the final approach to pure methane must be done at a relatively low temperature.

If it is assumed that the solid deposit is not graphite, but has the thermodynamic properties of "Dent" carbon, the situation is quite a bit different. At lower temperatures considered, "Dent" carbon is much less likely to be deposited than graphite, as indicated by the curve for  $600^\circ K$  in Figure V. As the temperature increases, the behavior of "Dent" carbon approaches that of graphite, and the carbon deposition region becomes greater. At approximately  $1100^\circ K$ , the curves for "Dent" carbon and graphite are the same. At higher temperatures, it is assumed that "Dent" carbon and graphite also behave identically in regards to deposition.

Since the effects of temperature on reactions 3 and 4 are in opposite directions, the different temperature curves also intersect, as is the case for graphite.

If it is assumed that the deposition of carbon is governed by the thermochemistry of "Dent" carbon, rather than graphite, it is obvious that there is a much greater region where deposition will not take place.

#### Equilibrium Compositions and Heating Value

The preceding discussion has been mostly confined to the carbon deposition curves as a function of temperature, pressure and initial composition. Also of interest, especially for methane synthesis, is the composition and heating value of the equilibrium gas mixture. It is desirable to produce a gas with a high heating value, which implies a high concentration of  $\text{CH}_4$ , and a low concentration of the other species. Of particular interest are the concentrations of  $\text{H}_2$  and  $\text{CO}$  as these generally are the valuable raw materials. Also, by custom it is desirable to maintain a  $\text{CO}$  concentration of less than 1 percent. The calculated heating values are reported according to the custom in the gas industry, which is based on a cubic foot at 30" Hg and 60°F, saturated with water vapor (11). Furthermore, it is calculated and reported for a  $\text{CO}_2$  and  $\text{H}_2\text{O}$  free gas as these components may be removed from the mixture after the final chemical reaction. Concentrations of  $\text{CH}_4$ ,  $\text{CO}$  and  $\text{H}_2$  are also reported on a  $\text{CO}_2 - \text{H}_2\text{O}$  free basis.

The higher heating value is plotted on the composition coordinate in Figure VI. These curves are for 50 atm and 700°K. The contours of constant heating value increase uniformly in the direction of pure methane. These contours, of course, are very similar to the contours of  $\text{CH}_4$  concentration, which are indicated in Figure VII, for the same conditions, 50 atm and 700°K.

Hydrogen concentration contours for 50 atm and 700°K are shown in Figure VIII. These contours indicate that there is appreciable unreacted hydrogen after equilibrium is obtained, and it is clear that multiple reaction stages are required to approach pure methane.

Carbon monoxide concentration contours are shown in Figure IX for 50 atm and 700°K. These curves indicate that the  $\text{CO}$  leakage will not be high if equilibrium is obtained if the initial composition is near the stoichiometric line.



Figure X shows the effect of temperature on higher heating value,  $\text{CH}_4$ ,  $\text{H}_2$ , and  $\text{CO}$  concentrations for four different starting compositions, which are also indicated on Figure II. The four starting compositions are:

	Y	X	
1	.75	.25	stoichiometric
2	.8	.0	stoichiometric
3	.7	.1	hydrogen deficient
4	.8	.05	hydrogen rich

In this context, "stoichiometric" implies any composition point on the line connecting pure water and pure methane. These mixtures have an  $\text{H}_2/\text{CO}$  ratio of 3.0 and contain either excess water or methane. Thus, they are stoichiometric with respect to hydrogen and carbon monoxide according to reaction 1. Points falling below the line are deficient in hydrogen, and points above the line are hydrogen rich.

In Figure X-A and B, the heating value and methane concentration decrease as a function of temperature for all four starting compositions. Conversely, the hydrogen and carbon monoxide concentrations increase, as seen on Figures X-C and D. The  $\text{CO}$  leakage is about the same for the two stoichiometric points, but is considerably larger for the hydrogen deficient starting composition.

Figure XI shows the effect of pressure on higher heating value and equilibrium composition for the same four starting compositions indicated on Figure X, all for a temperature of  $700^\circ\text{K}$ . Generally, the effect of pressure decreases as the pressure increases, most of the change occurring in the region up to 200 atm. For all of the compositions, as well as the higher heating values, the curves for two stoichiometric and for the hydrogen deficient starting points are similar. A difference is noted for the starting composition which is hydrogen rich. This is more apparent on Figure XI because it is plotted on a larger scale than on Figure X.

#### General Discussion

Various schemes have been proposed in the literature for carrying out the methane synthesis reaction, some of which are in use (6, 12, 13, 14).

A major engineering problem is removing the large amount of heat generated during the synthesis and numerous ways of doing this have been considered. The reactor temperature may be controlled by recycling product gas, with or without the water being condensed, or by otherwise diluting the reacting mixture with an excess of any of the products or reactants. This effectively changes the overall mixture composition. In addition, the fresh feed composition is widely variable depending upon the source of the feed gas. However, the charts presented here are applicable to a gas of any composition and allow one to see immediately if the possibility of carbon deposition exists for any given temperature within the range of interest. On Figure V for example, it indicates that it is not possible to approach pure  $\text{CH}_4$  at a high temperature without depositing carbon, and in fact, that a catalyst with a high temperature capability is not universally useful, but depends on the starting composition of the mixture. In any event, the final stage of the reaction to approach pure  $\text{CH}_4$  must be carried out at a low temperature.

References

- (1) Joint Army-Navy-Air Force Thermochemical Table, 2nd Ed., June 1971.
- (2) Rossini, F. D., et.al., "Selected Values of Properties of Hydrocarbons, Nat. Bur. Standards, Circular C461, 1947.
- (3) Dent, J. F., Moignard, L. A., Blackbraun, W. H., Herbden, D., "An Investigation into the Catalytic Synthesis of Methane by Town Gas Manufacture", 49th Report of the Joint Research Committee of the Gas Research Board and the University of Leeds, GRB20, 1945.
- (4) Pursley, J. A., R. R. White and C. Sliepcevich, Chem. Eng. Prog. Symposium Series, Vol. 48, No. 4, Reaction Kinetics, pp. 51-58, 1958.
- (5) Lunde, P. J. and F. L. Kester, Ind. Eng. Chem., Proc. Des. Develop., 13, No. 1, 1974.
- (6) Mills, G. A. and F. W. Steffgen, Catalysis Reviews, 8, No. 2, 159-210 (1973).
- (7) Greyson, M., in Catalysis, (P. H. Emmet, Ed.), 4, Chapter 6, 1956, Reinhold, N. Y.
- (8) Lee, A. L., H. L. Feldkirchner and D. G. Tajbl, "Methanation of Coal Hydrogasification", ACS Div. Fuel Chem. Preprints, 14, No. 4, Part I, 126-142, September, 1970.
- (9) Wen, C. Y., P. W. Chen, K. Kato and A. F. Galli, "Optimization of Fixed Bed Methanation Processes", ACS Div. Fuel Chemistry Preprints, 14, No. 3, 104-163, September, 1970.
- (10) Forney, A. J. and J. P. McGee, "The Synthane Process", Fourth AGA Pipeline Gas Symposium, Chicago, 1972.
- (11) McClahahan, D. N., Oil & Gas Journal, Feb. 20, 1967, pp. 84-90.
- (12) Greyson, M., et.al., U. S. Bureau of Mines, Rept. of Invest., 6609 (1965).
- (13) Forney, A. J. and W. P. Haynes, "The Synthane Coal to Gas Process: A Progress Report", ACS Div. Fuel Chem. Preprints, September, 1971.
- (14) Schoubye, P. J., Catalysis, 18, (1), 118 (1970).

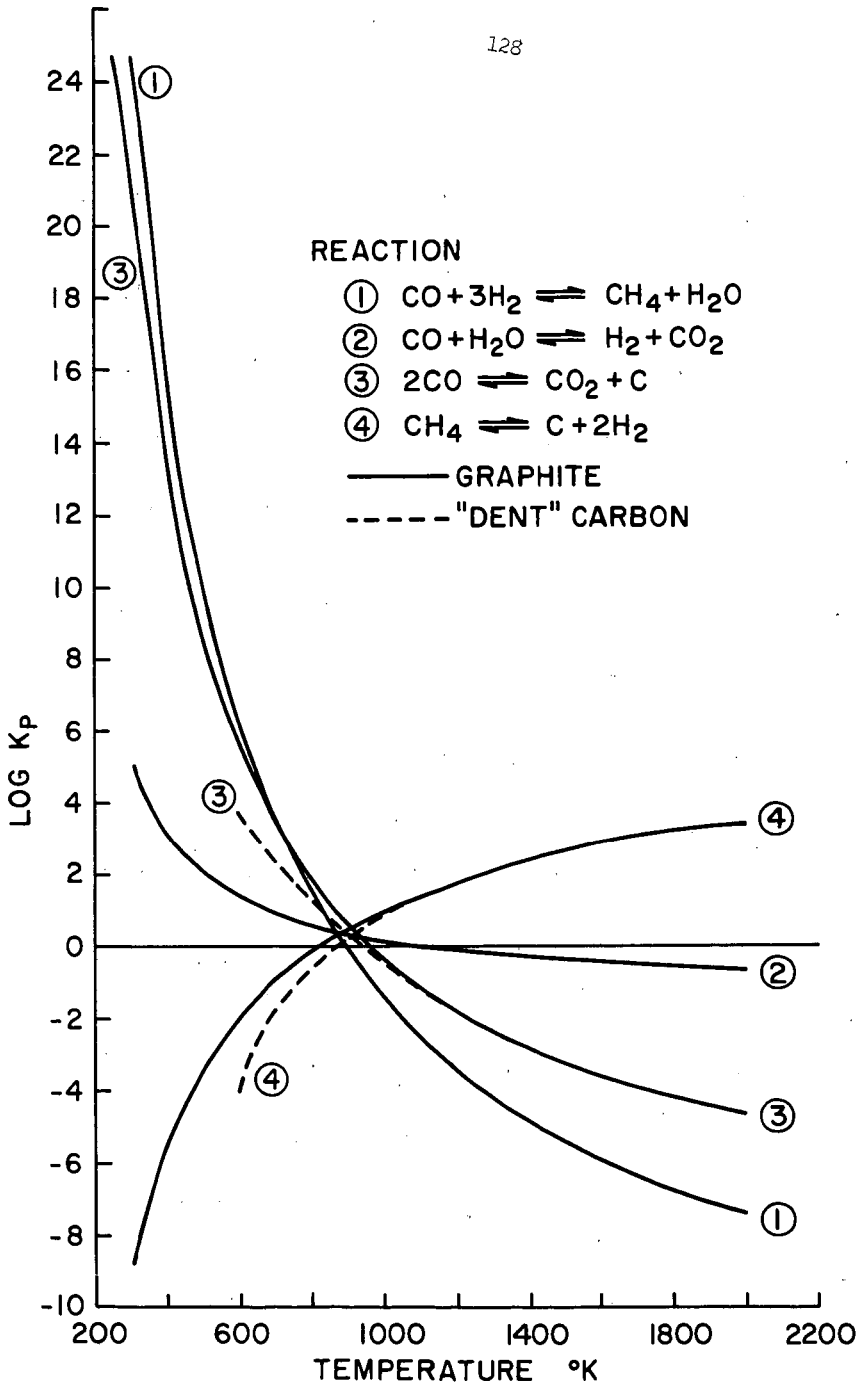


FIGURE I -EQUILIBRIUM CONSTANTS  
 AS A FUNCTION OF  
 TEMPERATURE

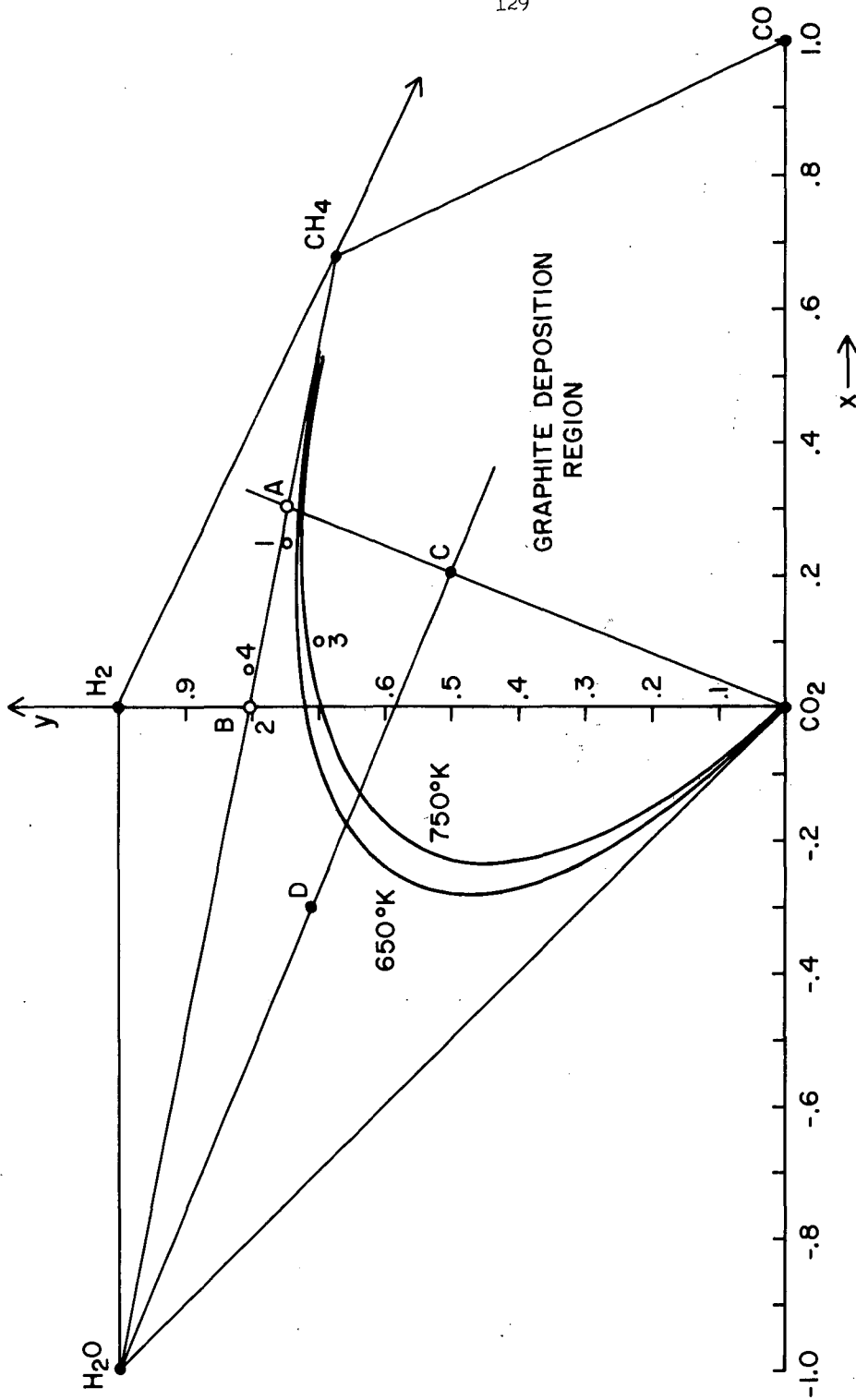


FIGURE II - GRAPHITE DEPOSITION AS A FUNCTION OF COMPOSITION AND TEMPERATURE 30 ATM

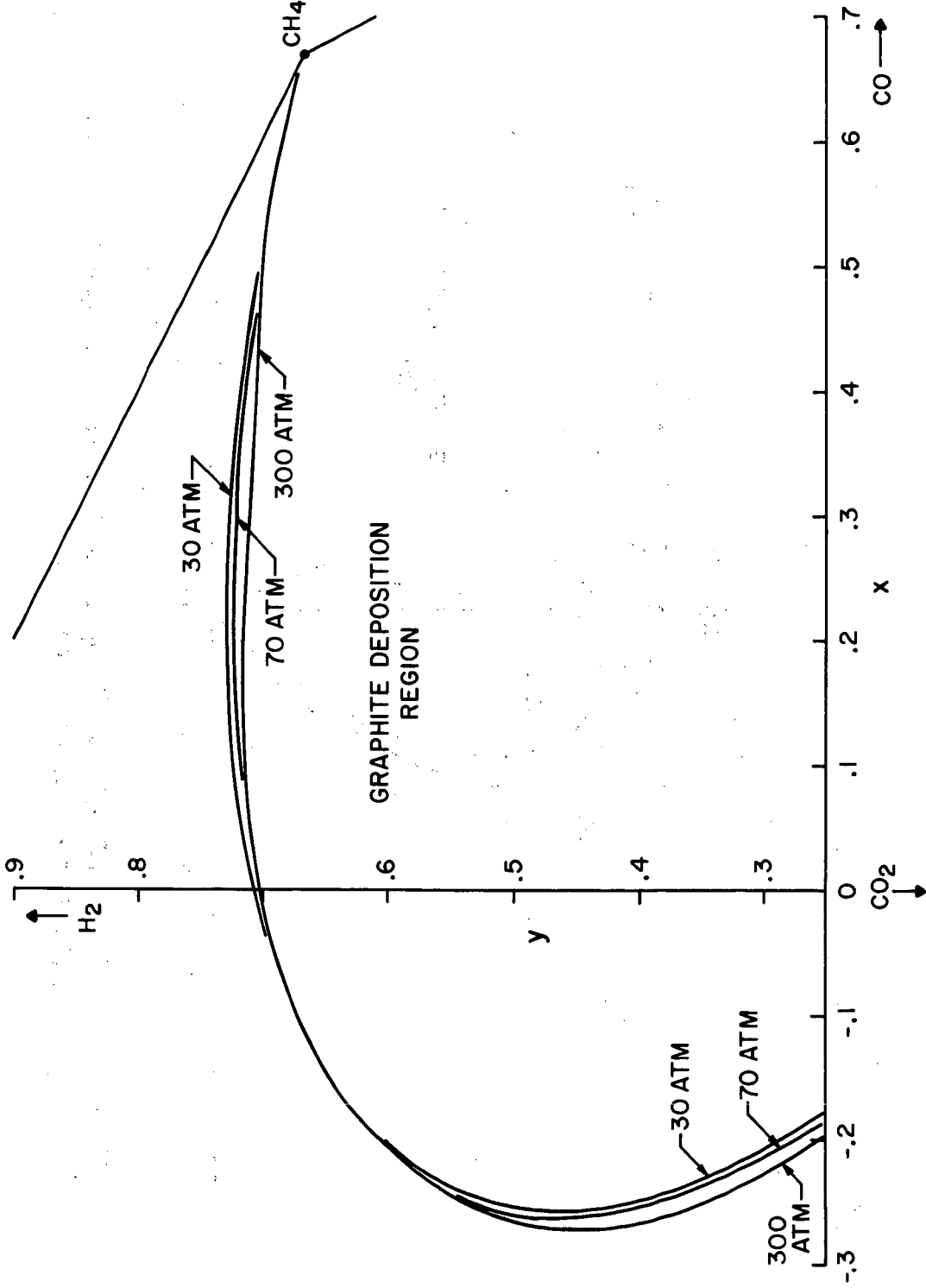


FIGURE III - EFFECT OF PRESSURE & COMPOSITION ON GRAPHITE DEPOSITION 700°K

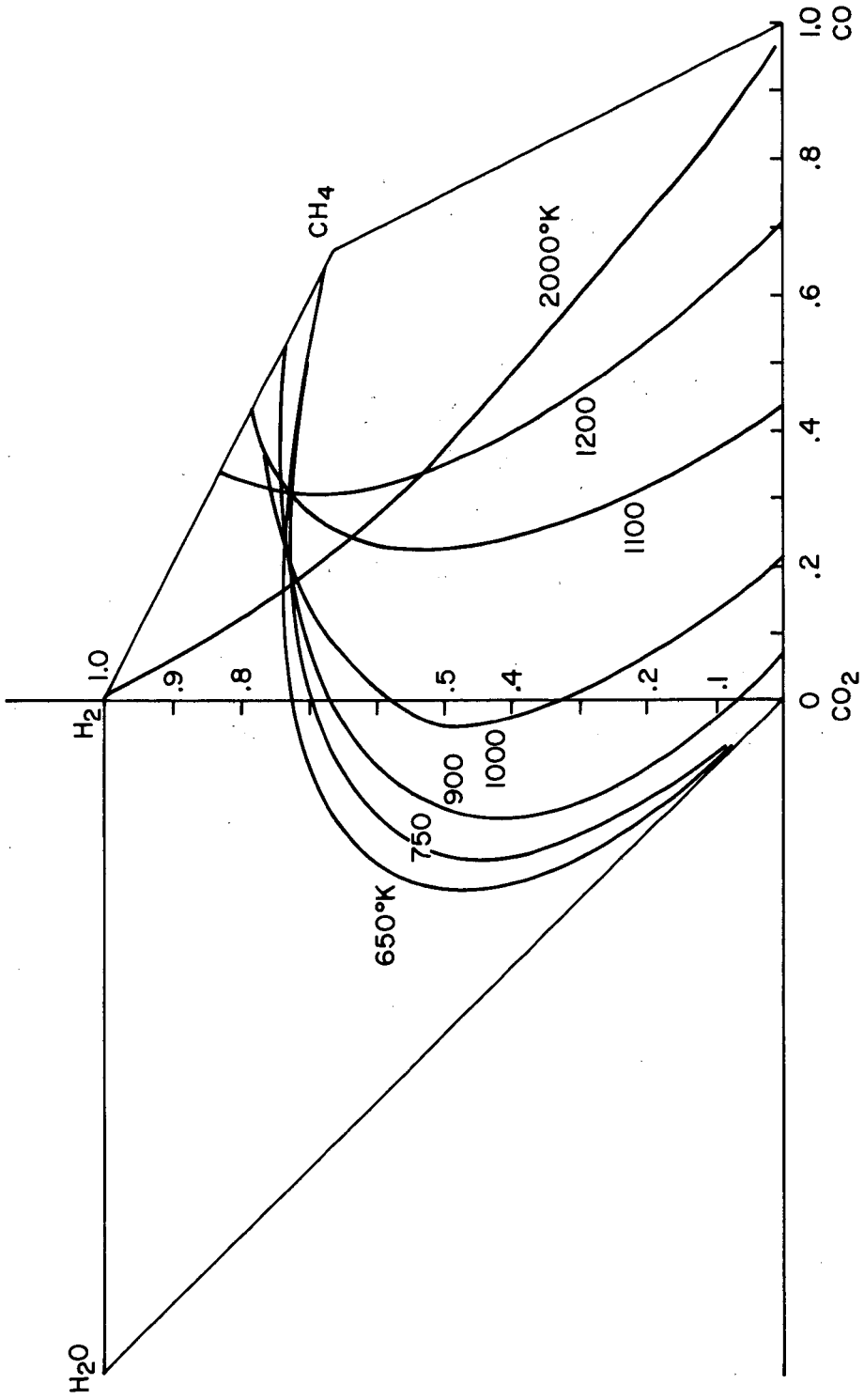


FIGURE IV - GRAPHITE DEPOSITION AT 30 ATM 650°K-2000°K

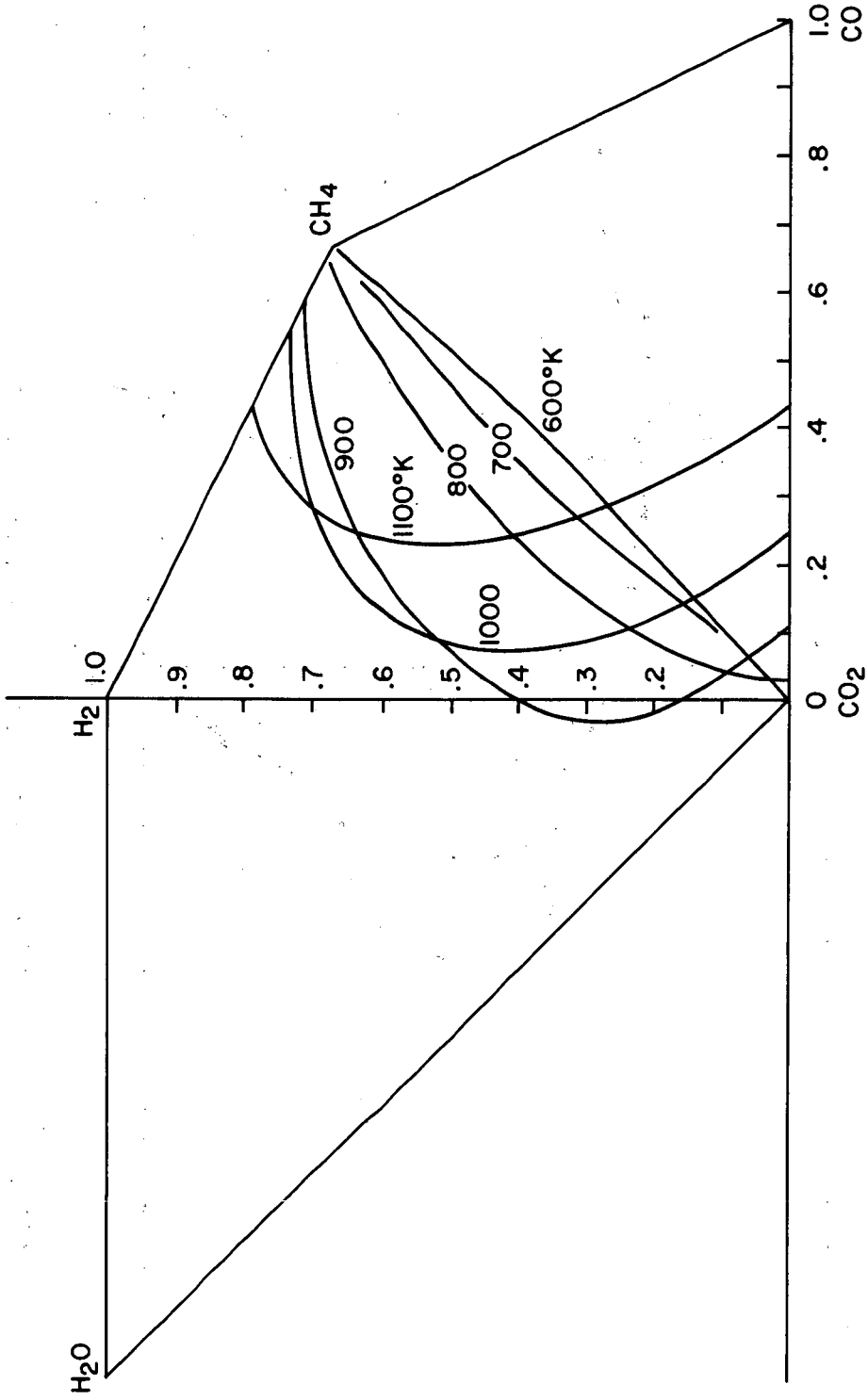


FIGURE V - DEPOSITION OF "DEND" CARBON 30 ATM



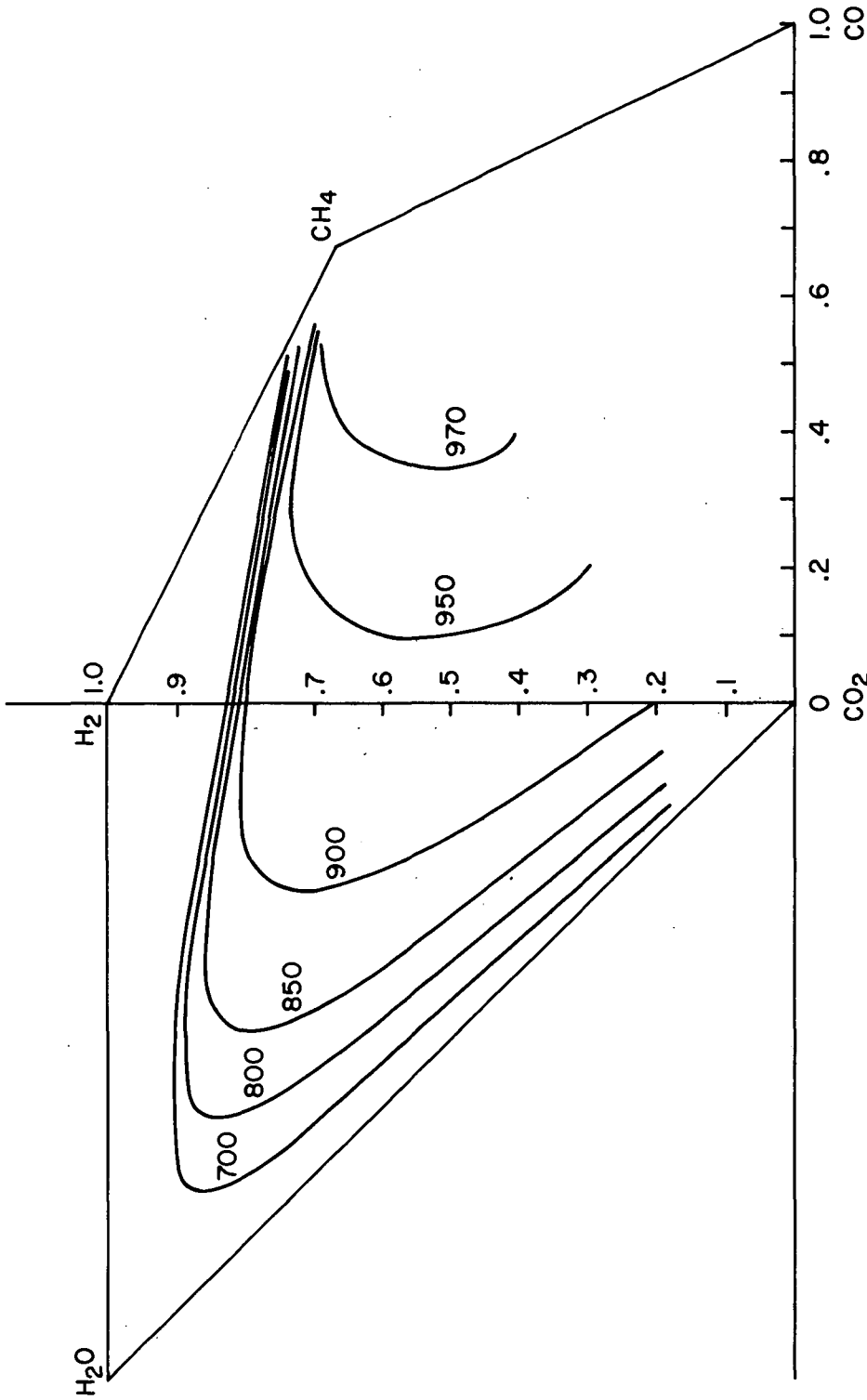


FIGURE VI - HIGHER HEATING VALUE OF  $\text{CO}_2$ ,  $\text{H}_2\text{O}$  FREE EQUILIBRIUM MIXTURES AS A FUNCTION OF STARTING COMPOSITION  
50 ATM, 700°K

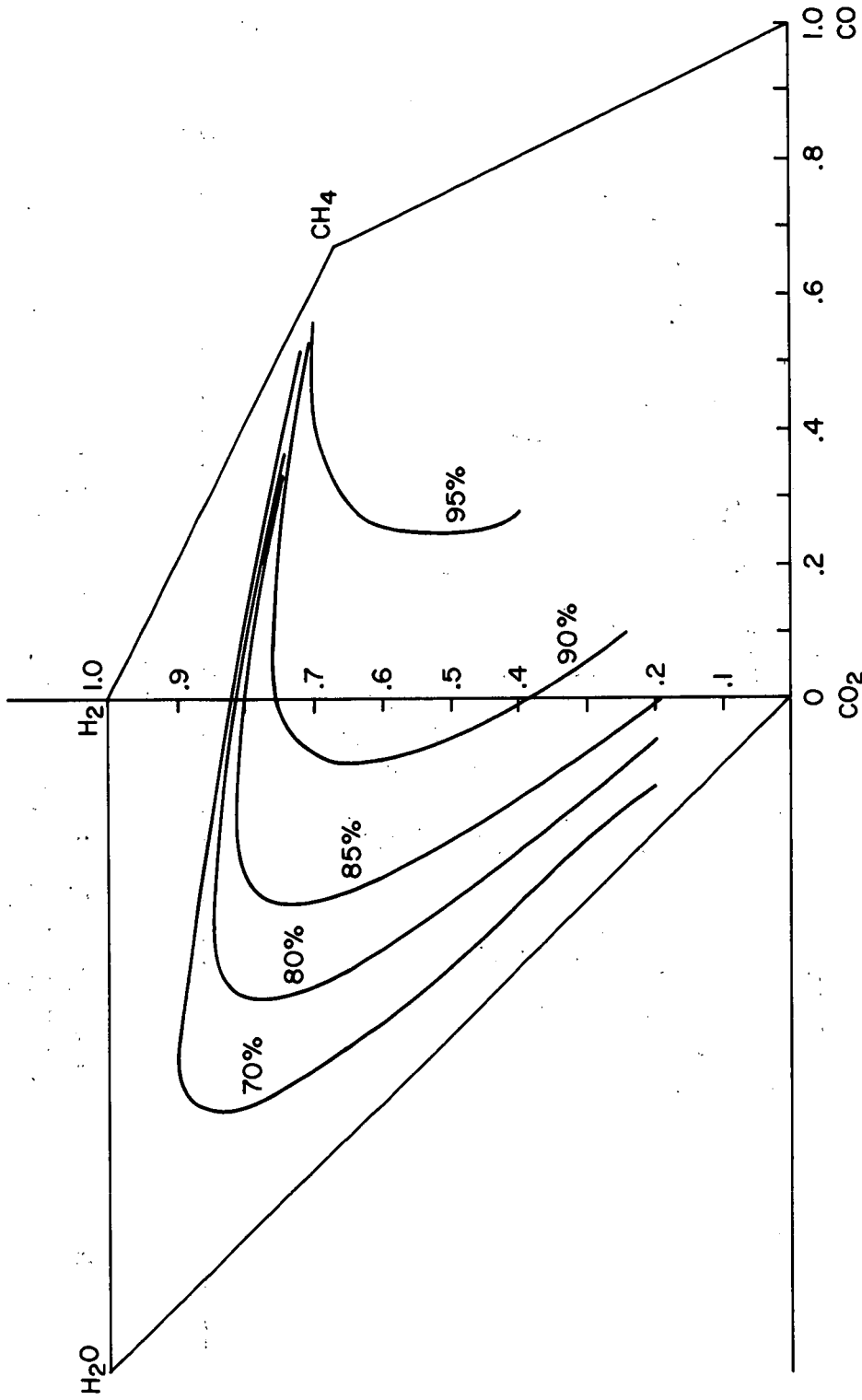


FIGURE VII -  $\text{CH}_4$  CONCENTRATION OF EQUILIBRIUM MIXTURES  
50 ATM, 700°K

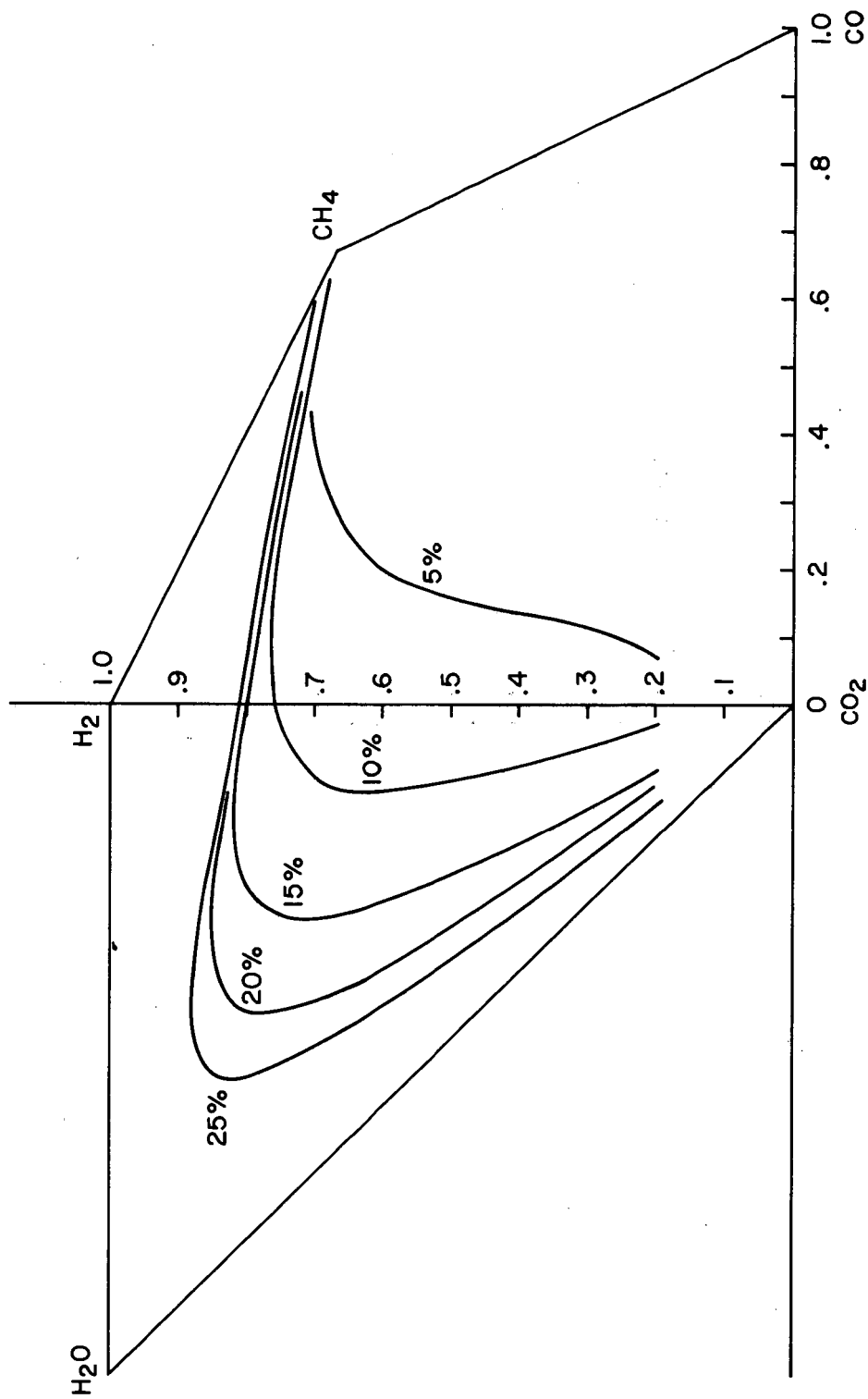


FIGURE VIII - H<sub>2</sub> CONCENTRATION OF EQUILIBRIUM MIXTURES  
H<sub>2</sub>O & CO<sub>2</sub> FREE 50ATM, 700°K

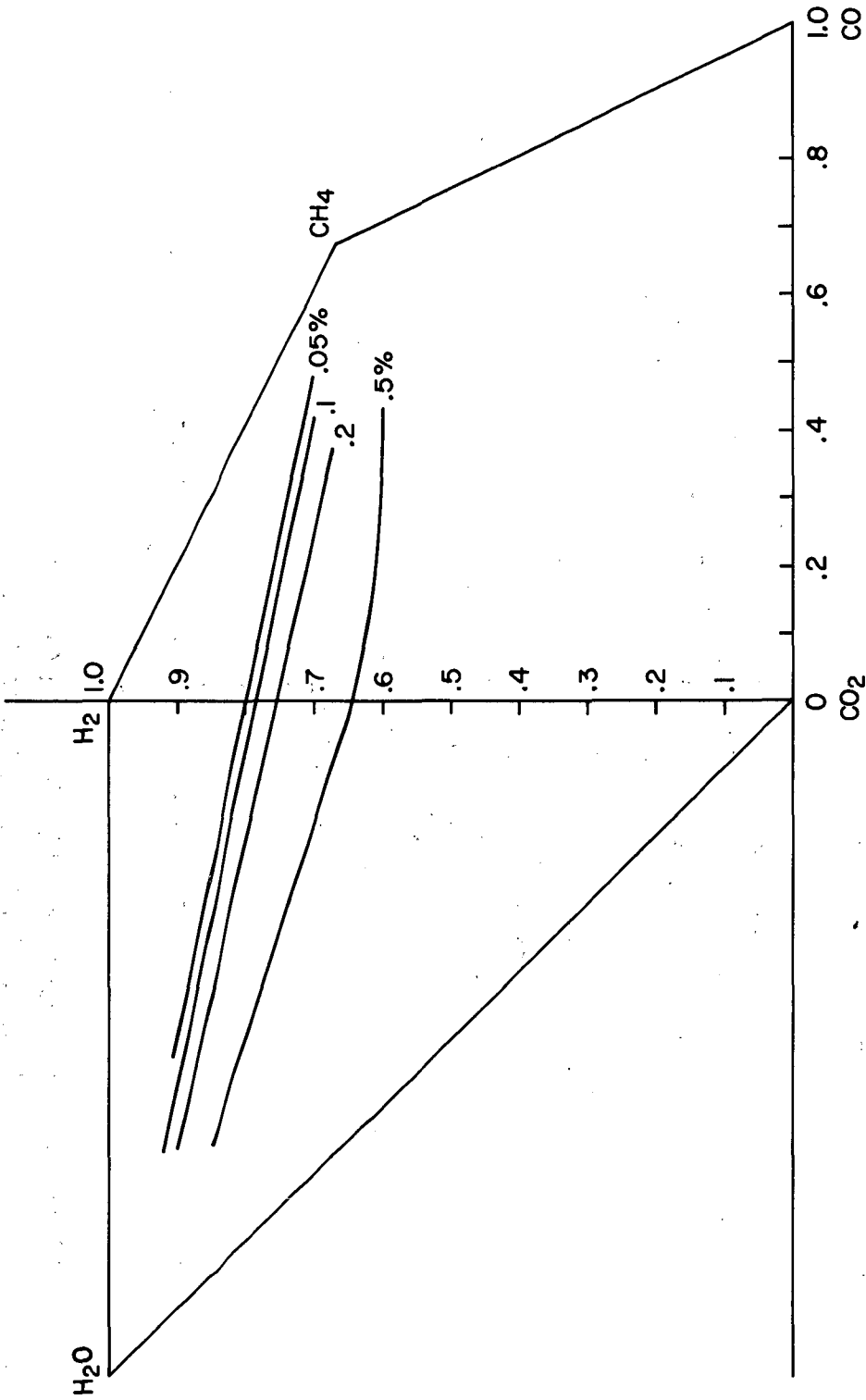


FIGURE IX - EQUILIBRIUM CO CONCENTRATION H<sub>2</sub>O & CO<sub>2</sub> FREE  
50 ATM, 700°K

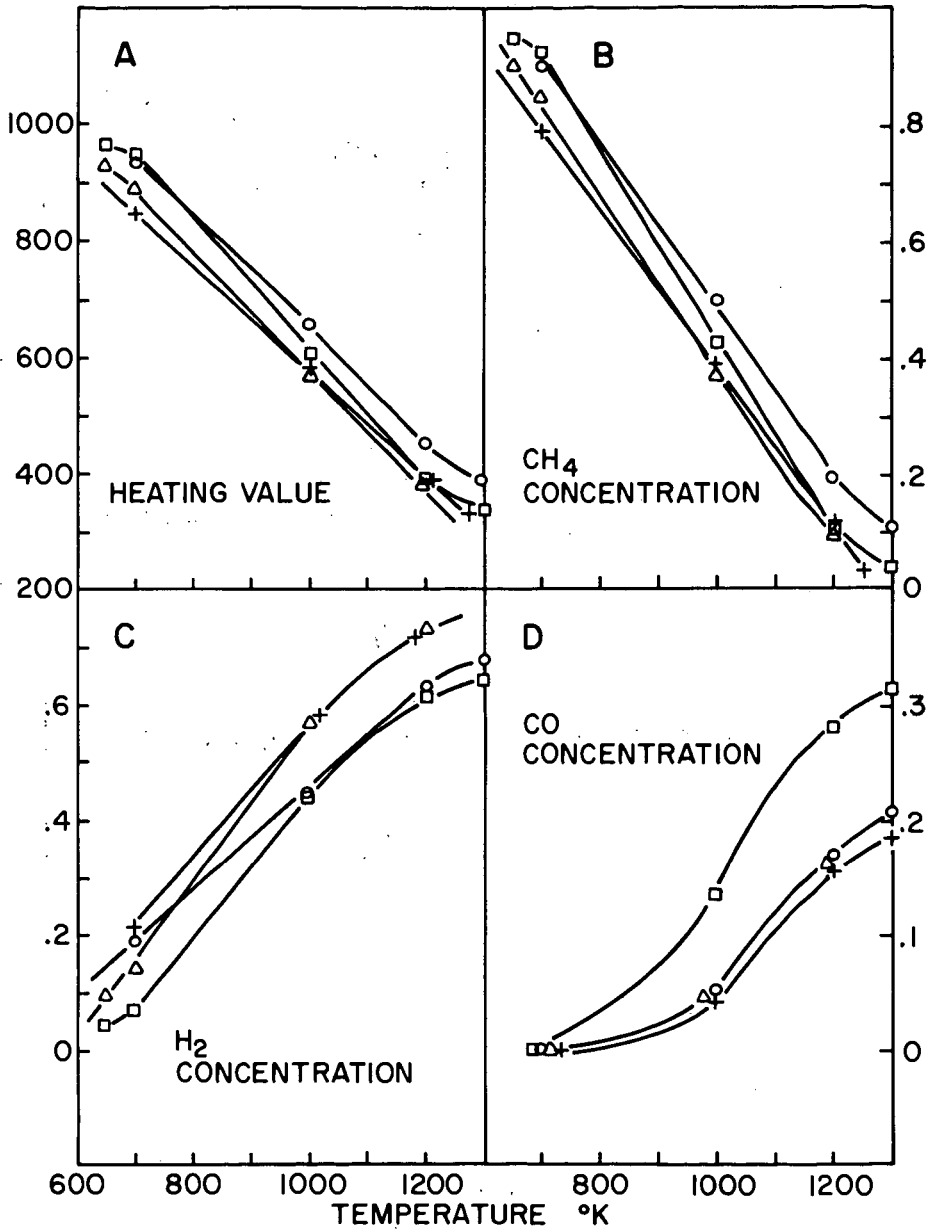


FIGURE X-EFFECT OF TEMPERATURE ON CONCENTRATION AT 50 ATM

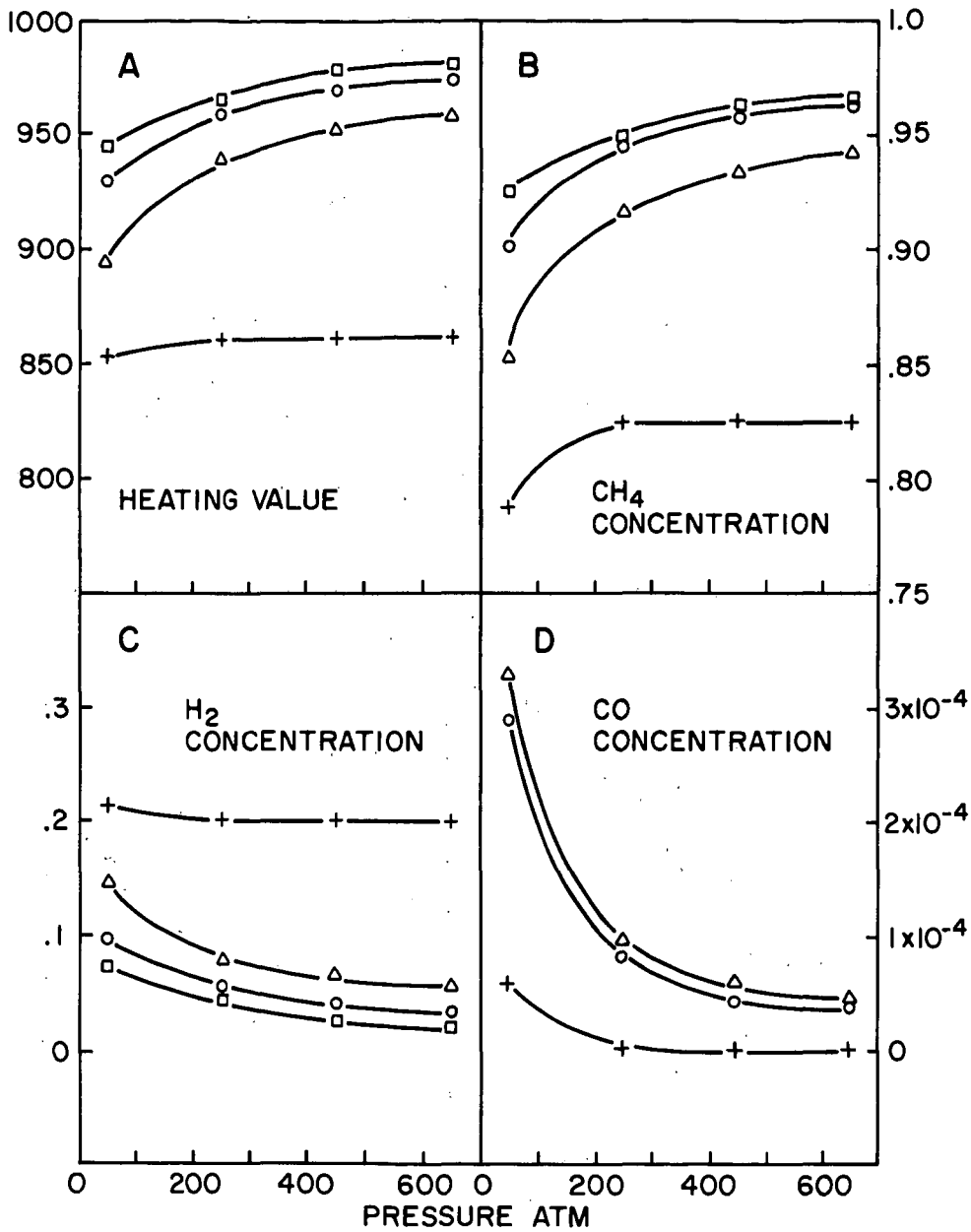


FIGURE XI-EFFECT OF PRESSURE ON  
CONCENTRATION AT 700°C

	y	x
○	.75	.25
△	.8	0
□	.7	.1
+	.8	.05